

# A Novel Local Pattern Descriptor—Local Vector Pattern in High-Order Derivative Space for Face Recognition

Kuo-Chin Fan and Tsung-Yung Hung

**Abstract**—In this paper, a novel local pattern descriptor generated by the proposed local vector pattern (LVP) in high-order derivative space is presented for use in face recognition. Based on the vector of each pixel constructed by computing the values between the referenced pixel and the adjacent pixels with diverse distances from different directions, the vector representation of the referenced pixel is generated to provide the 1D structure of micropatterns. With the devise of pairwise direction of vector for each pixel, the LVP reduces the feature length via comparative space transform to encode various spatial surrounding relationships between the referenced pixel and its neighborhood pixels. Besides, the concatenation of LVPs is compacted to produce more distinctive features. To effectively extract more detailed discriminative information in a given subregion, the vector of LVP is refined by varying local derivative directions from the  $n$ th-order LVP in  $(n - 1)$ th-order derivative space, which is a much more resilient structure of micropatterns than standard local pattern descriptors. The proposed LVP is compared with the existing local pattern descriptors including local binary pattern (LBP), local derivative pattern (LDP), and local tetra pattern (LTrP) to evaluate the performances from input grayscale face images. In addition, extensive experiments conducting on benchmark face image databases, FERET, CAS-PEAL, CMU-PIE, Extended Yale B, and LFW, demonstrate that the proposed LVP in high-order derivative space indeed performs much better than LBP, LDP, and LTrP in face recognition.

**Index Terms**—Local pattern descriptors, local binary pattern (LBP), local derivative pattern (LDP), local tetra pattern (LTrP), local vector pattern (LVP), comparative space transform (CST), face recognition.

## I. INTRODUCTION

FACE recognition attracts extensive attention recently in real-world applications [1]–[4]. In the scope of face recognition, it is admitted that face feature description significantly affects the recognition performance. More specifically, the three critical issues for developing a good face descriptor are: (1) maximize the margin between inter-person, (2) minimize the correlation between intra-person, and (3) can be extracted with low computational cost from original input data. However, a good recognition result can not be anticipated by

Manuscript received June 12, 2013; revised December 14, 2013 and April 14, 2014; accepted April 22, 2014. Date of publication May 2, 2014; date of current version May 27, 2014. The associate editor coordinating the review of this manuscript and approving it for publication was Prof. Joseph P. Havlicek.

The authors are with the National Central University, Taoyuan County 320, Taiwan (e-mail: kcfan@csie.ncu.edu.tw; ericchat119@gmail.com).

Color versions of one or more of the figures in this paper are available online at <http://ieeexplore.ieee.org>.

Digital Object Identifier 10.1109/TIP.2014.2321495

using unsatisfactory face features, even though adopting the optimum classifier. The existing face descriptions attempt to incorporate and balance the above criteria to produce more prominent recognition results.

Primarily, the desirable components of well-recognized face features in face recognition system are comprised mainly of local pattern descriptors [5]–[11], Eigenface [12], Fisherface [13], and manifold-based learning methods [14]–[17]. These methods are inclined to effectively extract the representation and discriminate classes from original input images. In particular, the importance of local pattern descriptors has been well recognized in face recognition because they can successfully and effectively represent the spatial structure information of an input image to generate distinguishing local features, such as local binary pattern (LBP) [18]–[21] which has been successfully applied to facial application for achieving good recognition results permitted with computational simplicity as well as low-dimensional space requirements.

Generally, a good local pattern descriptor is desired to extract discriminative and robust features from original input images. In face recognition, LBP achieves much better performance comparing with Eigenface and Fisherface. The idea of LBP is to divide a face image into sub-regions which include the compositions of micropatterns [21]. To generate a micropattern, each pixel is encoded based on the relationship between the referenced pixel and its neighborhoods, which can be modeled by the statistical histogram to represent the potential texture information (e.g., spots, lines, corners). On the other hand, LBP can also be considered as the non-directional first-order circular derivative local pattern which is used to concatenate binary comparative results for generating the micropatterns according to the extended definition from the local derivative pattern (LDP) [22]. Derived from the LBP, Zhang *et al.* proposed the high-order derivative descriptor for face representation that can more successfully capture the discriminative information than the LBP [22]. The reason is that the first-order derivative pattern fails to combine the relationship of neighborhoods to extract more detailed information. In the investigation, the LDP encodes the turning points or the monotonous ones to the two distinct values (“1” or “0”) by comparing the derivative values between the referenced pixel and its local neighborhoods in a given high-order derivative direction. Different from LDP, Murala *et al.* proposed the local tetra pattern (LTrP) to extend the two distinct values to four distinct values by using the two

high-order derivative direction patterns for generating more distinguishing information [23]. However, the LTrP encodes the four tetra patterns with the quadrant of the referenced pixel, while the other tetra patterns are encoded with “0” which possibly loses the potential texture information. It leads to both high redundancy and feature length increasing which are considered as critical issues for developing an effective local pattern descriptor. This observation hence motivates us to solve the problems of the LTrP to improve the performance for use in our face recognition application.

In this paper, we propose a novel pattern descriptor, called local vector pattern (LVP), for use in face recognition. We mainly aim at enhancing the proposed method with respect to the aforementioned problems (high redundancy and feature length increasing). To resolve these two problems, we develop a novel vector representation by calculating the various directions with diverse distances to represent the 1D direction and structure information of the face texture. Based on the vector representation, the LVP encodes various pairwise directions of vector as a facial descriptor to strengthen the structure of micropatterns. Moreover, we develop a novel coding scheme, comparative space transform (CST), in LVP encoding to encode a pairwise direction of vector for reducing the feature length and high redundancy resulting from LTrP. Furthermore, the proposed CST uses a designed dynamic linear decision function to suppress the slight noise influence, such as intensity change in a flat surface. In our work, the LVP can also be applied in various high-order derivative spaces to refine the vector representation for obtaining a more compact and discriminative local pattern descriptor. Hence, the first-order LVP can be considered as the non-directional derivative local pattern, and the second-order LVP refines the vector to obtain 2D direction information of local structure in various first-order derivative spaces. Consequently, the  $n^{th}$ -order LVP is a general form representing a local pattern descriptor which inherently generates more detailed information from a given local structure. According to our observation, like the LBP, the LVP can be modeled by statistical histogram to represent the generated spatial distribution of the LVP micropatterns. In addition, the use of more directional information makes the high-order LVP exhibit better performance in various experimental results comparing to a set of similar methods (the LBP, the LDP, and the LTrP).

The rest of this paper is organized as follows. Section II briefly discusses the related works. The proposed local vector pattern (LVP) and comparative space transform (CST) coding scheme are presented in Section III. The extension of LVP in high-order derivative space is addressed in Section IV. Experimental results conducted on FERET [24], CAS-PEAL [25], CMU-PIE [26], Extended Yale B [27], [28] and LFW [29] databases in the comparison study are demonstrated in Section V. Finally, conclusions are given in Section VI.

## II. LOCAL PATTERN DESCRIPTORS

In this section, a brief review of several state-of-the-art local pattern descriptors including LBP, LDP, and LTrP are given

$G_{4,1}$	$G_{3,1}$	$G_{2,1}$
$G_{5,1}$	$G_c$	$G_{1,1}$
$G_{6,1}$	$G_{7,1}$	$G_{8,1}$

Fig. 1. The 8-neighborhood surrounding  $G_c$ .

to describe the properties of these methods for encoding the micropatterns.

### A. Local Binary Pattern

The definition of texture is extensively investigated and utilized in micropatterns for modeling the texture structure. The LBP descriptor is a general definition which is introduced as a rotation invariant texture measure with both computational simplicity and high discriminative capability in various comparative studies [20], [21]. Moreover, the basic LBP is constantly used to extract the discriminative feature that is encoded through the binomial concatenation of the relationship between a given referenced pixel  $G_c$  and its neighborhoods with radius  $R$  based on the following equation. ( $R$  is the radius between the referenced pixel and its neighborhood pixels, which is set as unit in the following methods for comparison sake. Accordingly, the number of neighborhood pixels of the referenced pixel  $P$  is set as 8 as shown in Fig. 1.)

$$\begin{aligned} LBPP_{P,R}(G_c) = \{ & s_1(I(G_{1,R}), I(G_c)), s_1(I(G_{2,R}), I(G_c)), \\ & \dots, s_1(I(G_{p,R}), I(G_c)) \} |_{p=1,2,\dots,P; R=1} \end{aligned} \quad (1)$$

where  $G_{p,R}$  is one of 8-neighborhoods of the referenced pixel with unit-radius, and  $p$  is the index of the neighborhoods surrounding referenced pixel  $G_c$  in a given local sub-region  $I$ . The label of each neighborhood is decided by calculating the coding function  $s_1(\cdot, \cdot)$  with both referenced pixel and neighborhood pixel, called *threshold function*, which can be formulated as

$$s_1(I(G_{p,R}), I(G_c)) = \begin{cases} 1, & \text{if } (I(G_{p,R}) - I(G_c)) \geq 0 \\ 0, & \text{else} \end{cases} \quad (2)$$

where the output of  $s_1(\cdot, \cdot)$  represents the binary gradient direction. Furthermore, the local features of the distribution of local sub-region can be modeled as the edges, spots, corners, and other local features.

### B. Local Derivative Pattern

The LBP can be considered as a general definition to generate micropatterns in local neighborhoods. On the other hand, the LBP is basically a non-directional first-order local pattern descriptor of LDP. In a general formulation, the LDP expands the LBP with the high-order derivative direction variations for extracting more detailed discriminative features [22]. For encoding the  $n^{th}$ -order LDP, the  $(n-1)^{th}$ -order derivatives along  $0^\circ, 45^\circ, 90^\circ$  and  $135^\circ$  directions are denoted as  $I_a^{n-1}(G_c)$

where  $\alpha = 0^\circ, 45^\circ, 90^\circ$  and  $135^\circ$ , which are pre-calculated separately based on

$$I_{0^\circ}^{n-1}(G_c) = I_{0^\circ}^{n-2}(G_{1,R}) - I_{0^\circ}^{n-2}(G_c) \quad (3)$$

$$I_{45^\circ}^{n-1}(G_c) = I_{45^\circ}^{n-2}(G_{2,R}) - I_{45^\circ}^{n-2}(G_c) \quad (4)$$

$$I_{90^\circ}^{n-1}(G_c) = I_{90^\circ}^{n-2}(G_{3,R}) - I_{90^\circ}^{n-2}(G_c) \quad (5)$$

$$I_{135^\circ}^{n-1}(G_c) = I_{135^\circ}^{n-2}(G_{4,R}) - I_{135^\circ}^{n-2}(G_c). \quad (6)$$

Then, the  $n^{\text{th}}$ -order LDP,  $LDP_{P,R,\alpha}^n(G_c)$ , in  $\alpha$  derivative direction at  $G_c$  is encoded as

$$\begin{aligned} LDP_{P,R,\alpha}^n(G_c) &= \{s_2(I_\alpha^{n-1}(G_{1,R}), I_\alpha^{n-1}(G_c)), \\ &\quad s_2(I_\alpha^{n-1}(G_{2,R}), I_\alpha^{n-1}(G_c)), \dots, \\ &\quad s_2(I_\alpha^{n-1}(G_{p,R}), I_\alpha^{n-1}(G_c))\}|_{p=1,2,\dots,P;R=1} \end{aligned} \quad (7)$$

where the output of  $s_2(\cdot, \cdot)$  represents the spatial relationship between the referenced pixel and its neighborhoods in a given derivative direction. Typically, the spatial relationship between two different neighborhood pixels can be classified into two categories: the turning point is labeled as “1” in the broad sense and monotonically increasing or decreasing is labeled as “0”. In other words,  $s_2(\cdot, \cdot)$  determinates the types of 1D spatial relationship transitions and also labels the neighborhood pixels of the referenced pixel into a binary code as

$$s_2(I_\alpha^{n-1}(G_{p,R}), I_\alpha^{n-1}(G_c)) = \begin{cases} 1, & \text{if } (I_\alpha^{n-1}(G_{p,R}) \times I_\alpha^{n-1}(G_c)) \leq 0 \\ 0, & \text{else.} \end{cases} \quad (8)$$

Finally, the  $n^{\text{th}}$ -order LDP,  $LDP_{P,R}^n(G_c)$  at  $G_c$ , is defined as the concatenation of the four directional LDPs

$$LDP_{P,R}^n(G_c) = \{LDP_{P,R,\alpha}^n(G_c)|\alpha = 0^\circ, 45^\circ, 90^\circ, 135^\circ\}. \quad (9)$$

The detailed discussion can be found in [22].

### C. Local Tetra Pattern

Murala *et al.* proposed the LTrP for image retrieval [23]. Typically, the LDP is encoded based on the relationship between the referenced pixel and its neighborhoods with single high-order derivative direction which is a general concatenate comparison between the referenced pixel and its neighborhoods to obtain a micropattern in local sub-region. Murala *et al.* found that the 1D spatial relationship of the LDP can be extended to the 2D spatial relationship in terms of the LTrP adopting both the horizontal and vertical high-order derivative directions. Based on the observation, one high-order derivative direction in the scheme can be expanded to four distinct values with exponential growth. As a result, the LTrP encoded with four distinct values by using two high-order derivative directions can extract more detailed discriminative information than the LDP which only considers single high-order derivative direction with two distinct values. In order to encode the  $n^{\text{th}}$ -order LTrP, the  $(n-1)^{\text{th}}$ -order derivatives along  $0^\circ$  and  $90^\circ$  directions have to be pre-calculated similar to (3)

and (5). The quadrant representation of the distinct value at  $G_c$  can be defined as

$$I_{Dir.}^{n-1}(G_c) = \begin{cases} 1, & I_{0^\circ}^{n-1}(G_c) \geq 0 \text{ and } I_{90^\circ}^{n-1}(G_c) \geq 0 \\ 2, & I_{0^\circ}^{n-1}(G_c) < 0 \text{ and } I_{90^\circ}^{n-1}(G_c) \geq 0 \\ 3, & I_{0^\circ}^{n-1}(G_c) < 0 \text{ and } I_{90^\circ}^{n-1}(G_c) < 0 \\ 4, & I_{0^\circ}^{n-1}(G_c) \geq 0 \text{ and } I_{90^\circ}^{n-1}(G_c) < 0 \end{cases} \quad (10)$$

where the output of  $I_{Dir.}^{n-1}(G_c)$  represents the quadrant of the  $G_c$  along  $0^\circ$  and  $90^\circ$  directions. The distinct values are expanded to four possible values, which provide better outcome comparing with LBP and LDP.

Then, the  $n^{\text{th}}$ -order LTrP,  $LTrP_{P,R}^n(G_c)$ , at  $G_c$  is encoded as

$$\begin{aligned} LTrP_{P,R}^n(G_c) &= \{s_3(I_{Dir.}^{n-1}(G_{1,R}), I_{Dir.}^{n-1}(G_c)), \\ &\quad s_3(I_{Dir.}^{n-1}(G_{2,R}), I_{Dir.}^{n-1}(G_c)), \dots, \\ &\quad s_3(I_{Dir.}^{n-1}(G_{p,R}), I_{Dir.}^{n-1}(G_c))\}|_{p=1,2,\dots,P;R=1} \end{aligned} \quad (11)$$

$$s_3(I_{Dir.}^{n-1}(G_{p,R}), I_{Dir.}^{n-1}(G_c)) = \begin{cases} I_{Dir.}^{n-1}(G_{p,R}), & \text{if } I_{Dir.}^{n-1}(G_{p,R}) \neq I_{Dir.}^{n-1}(G_c) \\ 0, & \text{else} \end{cases} \quad (12)$$

where  $s_3(\cdot, \cdot)$  is used to obtain the model of four quadrants of tetra patterns based on the quadrant of the referenced pixel. Afterwards, the tetra patterns are segregated into three binary patterns to reduce the feature length based on

$$\begin{aligned} LTrP_{P,R}^n|_{\widehat{Dir.} \setminus \{Dir.\}} &= s_4(LTrP_{P,R}^n(G_c))|_{\widehat{Dir.} \setminus \{Dir.\}} \end{aligned} \quad (13)$$

$$s_4(LTrP_{P,R}^n(G_c))|_{\widehat{Dir.} \in \widehat{Dir.}} = \begin{cases} 1, & \text{if } LTrP_{P,R}^n(G_c) = \widehat{Dir.} \\ 0, & \text{else} \end{cases} \quad (14)$$

where  $\widehat{Dir.}$  is a set which contains four quadrants except the quadrant of the referenced pixel and  $\widehat{Dir.}$  is one of the quadrants of the  $\widehat{Dir.}$ . The output of  $s_4(\cdot, \cdot)$  can be used to reconstruct the three binary patterns. Similarly, the other three tetra patterns are generated based on (13) and (14). Moreover, the magnitude of LBP is adopted to join with the concatenation of the four tetra patterns for encoding the complete local features of  $LTrP_{P,R}^n(G_c)$  [30]. The detailed discussion can be found in [23].

## III. THE PROPOSED LOCAL PATTERN DESCRIPTOR

According to the literature review in Section II, we observe that the LBP is a basic descriptor for extracting micropatterns without considering feasible neighboring relationship, the LDP only adopts the single derivative direction and loses potential information between derivative directions, and the LTrP generates micropatterns by using both horizontal and vertical derivative directions so that it produces high redundancy and feature length increasing. In consequence, we propose a novel local pattern descriptor, called Local Vector Pattern (LVP), to remedy the drawbacks existing in current local pattern descriptors. The LVP proposed in this paper generates

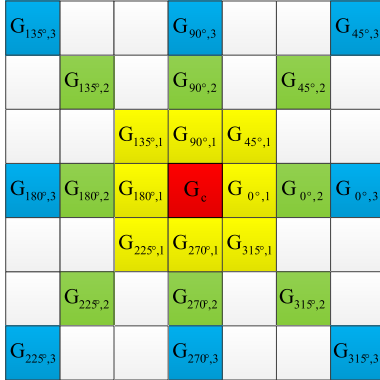


Fig. 2. Adjacent pixels of  $V_{\beta,D}(G_c)$  with different distances along each direction.

the micropatterns encoded through the pairwise directions of vector by using an effective coding scheme called Comparative Space Transform (CST) for successfully extracting distinctive information. In addition to the proposed LVP and CST, the histogram intersection method adopted in existing local pattern descriptors for evaluating the similarity between the spatial histograms of two distributions extracted from the LVP will also be addressed in this Section.

#### A. Local Vector Pattern

In our work, the key idea of the LTrP proposed in [23] is applied and improved to generate more discriminative features in our proposed LVP. Under the non-directional derivative preprocessing, the coding function of the LBP only considers the grayscale value of the referenced pixel and its neighborhoods and the LDP encodes the two distinct values (“1” or “0”) by comparing the single high-order derivative direction between the referenced pixel and its neighborhoods. As a result, the horizontal and vertical high-order derivative directions are adopted for generating the four quadrants in LTrP. That is the LTrP extends the LDP to encode the tetra patterns of the surrounding neighborhoods with the quadrant of the referenced pixel. In this paper, a novel vector representation is developed to represent the 1D direction and structure information of local texture by calculating the values between the referenced pixel and the adjacent pixels with diverse distances from different directions. Based on the vector representation, the LVP descriptor is proposed to provide various 2D spatial structures of micropatterns with various pairwise directions of vector of the referenced pixel and its neighborhoods. Moreover, the coding functions of micropatterns in LBP, LDP, and LTrP are investigated for extracting more detailed discriminative features by encoding the various pairwise directions of vector of micropatterns through the proposed CST. The proposed CST here encodes the pairwise directions of vector with two distinct values by using dynamic linear decision function to extract discriminative features.

Given a local sub-region  $I$ , the direction value of a vector is denoted as  $V_{\beta,D}(G_c)$  as illustrated in Fig. 2. Let  $G_c$  denote the referenced pixel marked with red in  $I$ ,  $\beta$  be the index angle of the variation direction, and  $D$  be the distance between the

referenced pixel and its adjacent pixels along the  $\beta$  direction. For illustration purpose, the distance  $D = 1$  is marked with yellow,  $D = 2$  is marked with green, and  $D = 3$  is marked with blue. The direction value of a vector at the referenced pixel  $G_c$  can be defined as

$$V_{\beta,D}(G_c) = (I(G_{\beta,D}) - I(G_c)). \quad (15)$$

When  $D = 1$ , the vector can be considered as the first-order derivative values of LDP and LTrP. When  $D > 1$ , the implicit characteristics of 1D direction information can be acquired.

The LVP,  $LVP_{P,R,\beta}(G_c)$ , in  $\beta$  direction of vector at  $G_c$  is encoded as

$$\begin{aligned} LVP_{P,R,\beta}(G_c) = & \{s_5(V_{\beta,D}(G_{1,R}), V_{\beta+45^\circ,D}(G_{1,R}), V_{\beta,D}(G_c), \\ & V_{\beta+45^\circ,D}(G_c)), s_5(V_{\beta,D}(G_{2,R}), \\ & V_{\beta+45^\circ,D}(G_{2,R}), V_{\beta,D}(G_c), V_{\beta+45^\circ,D}(G_c)), \\ & \dots, \\ & s_5(V_{\beta,D}(G_{p,R}), V_{\beta+45^\circ,D}(G_{p,R}), V_{\beta,D}(G_c), \\ & V_{\beta+45^\circ,D}(G_c))\}|_{p=1,2,\dots,P;R=1} \end{aligned} \quad (16)$$

where  $s_5(\cdot, \cdot)$  adopts transform ratio which is calculated with a pairwise direction of vector of the referenced pixel to transform the  $\beta$ -direction value of neighborhoods to  $(\beta + 45^\circ)$ -direction, which is used to compare with the original  $(\beta + 45^\circ)$ -direction value of neighborhoods for labeling the binary pattern of micropatterns. Therefore,  $s_5(\cdot, \cdot)$  can be formally defined as

$$\begin{aligned} & s_5(V_{\beta,D}(G_{p,R}), V_{\beta+45^\circ,D}(G_{p,R}), V_{\beta,D}(G_c), V_{\beta+45^\circ,D}(G_c)) \\ & = \begin{cases} 1, & \text{if } V_{\beta+45^\circ,D}(G_{p,R}) - \left( \frac{V_{\beta+45^\circ,D}(G_c)}{V_{\beta,D}(G_c)} \times V_{\beta,D}(G_{p,R}) \right) \geq 0 \\ 0, & \text{else.} \end{cases} \end{aligned} \quad (17)$$

Finally, the LVP,  $LVP_{P,R}(G_c)$ , at referenced pixel  $G_c$  is defined as the concatenation of the four 8-bit binary patterns LVPs.

$$LVP_{P,R}(G_c) = \{LVP_{P,R,\beta}(G_c) | \beta = 0^\circ, 45^\circ, 90^\circ, 135^\circ\}. \quad (18)$$

In order to extract more discriminative 2D spatial structures of micropatterns, the proposed local pattern descriptor encodes the LVPs by using the four pairwise directions of vector of the referenced pixel and its neighborhoods. Especially, each pairwise direction of vector of the referenced pixel generates the transform ratio which is used to design the weight vector of dynamic linear decision function for encoding the distinct 8-bit binary pattern of each LVP. Different from the LTrP in encoding the 96 ( $4 \times 3 \times 8$ )-bit (three 8-bit binary patterns for each tetra pattern) binary pattern which uses both horizontal and vertical high-order derivative directions, the LVP reduces the feature length from 96-bit binary pattern to 8-bit binary pattern. More precisely, the LVP can extract more detailed texture information than the LTrP by using the four pairwise directions of vector. As a result, the LVPs are concatenated to form as a 32 ( $4 \times 8$ )-bit binary pattern for each referenced pixel in the local sub-region.

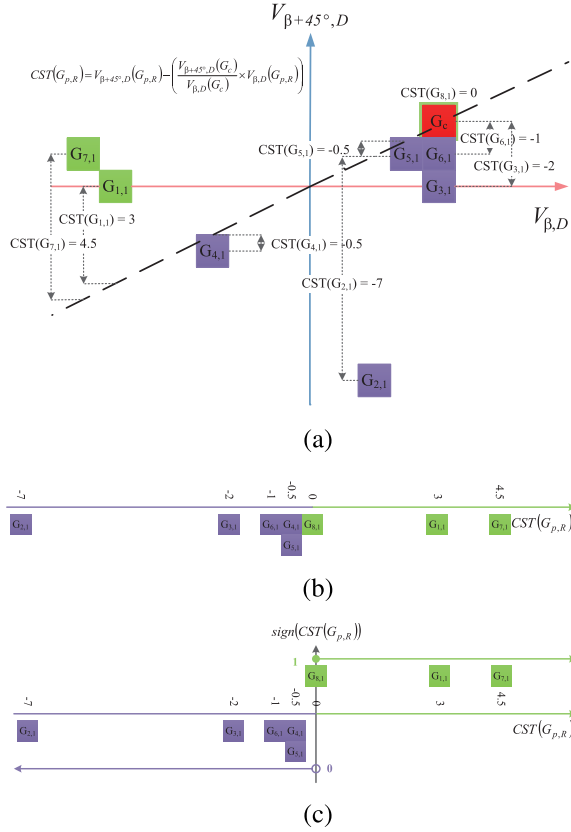


Fig. 3. Illustration of the proposed coding scheme in encoding the first-order LVP micropattern in direction  $\beta = 0^\circ$ . (a) The referenced pixel and its neighborhoods illustrated in 2D distribution, (b) the calculated CST values of neighborhood pixels illustrated in 1D distribution, (c) the use of sign function in encoding the neighborhoods. (a) Illustration of comparative space transform (CST). (b) CST values. (c) Sign function.

### B. Coding Scheme - Comparative Space Transform

The proposed coding scheme, Comparative Space Transform (CST), encodes the 8-bit binary code of each pixel and the concatenation of the encoded LVPs represents the 2D structures of micropatterns. In the previously proposed coding schemes, they pointed out that the complete binary code is sensitive to lighting changes of grayscale images by encoding the various derivative values [20]–[23]. In response to this observation, we introduce fundamental pattern recognition theorem to suppress the illumination influence for generating the distinct LVPs' binary code. Here, the dynamic linear decision function is developed for encoding each binary code of LVP which can be considered as the two-class problem in pattern recognition. One important issue of this problem is the design of decision function. In this paper, we design the weight vectors of dynamic linear decision function to separate the surrounding neighborhoods in order to encode the binary code. The pairwise direction of vectors of the referenced pixel and its neighborhoods provide valuable information in the 2D distribution. Fig. 3 illustrates the proposed coding scheme. Consider the added slight noise as shown in Fig. 3. When the direction values of neighborhoods switch over the positive and the negative directions, it can be observed that the binary code can

stay stable by using the proposed coding scheme while the previous coding methods may generate totally different code. For instance, the neighborhood pixel  $G_{7,1}$  can still be encoded as "1" even under the  $(\beta + 45^\circ)$ -direction value of  $G_{7,1}$  where the direction changes from positive to negative. Hence, the proposed CST can successfully suppress the slight noisy influence in grayscale images.

The coding schemes of the previous methods have several drawbacks in generating the specific code, especially under the illumination changes and noise influence in the face images. For example, LBP encodes the surrounding neighborhoods by using the grayscale value of the referenced pixel as a *threshold function* [20], [21]. If the grayscale values of the referenced pixel and its neighborhoods are similar, the *threshold function* is very sensitive to noise and will thereby encode different code that deteriorates the performance of accuracy immediately. Derived from the LBP, the LDP encodes the 1D spatial relationship between the referenced and its neighborhoods with single high-order derivative direction that can be considered as either the turning point or monotonically increasing or decreasing spatial relationship [22]. Extended from the LDP, the LTrP adopts both the horizontal and vertical high-order derivative directions to encode the 2D spatial relationship [23]. Similar to the problem occurring in LBP, the high-order derivative values of the neighborhoods are sensitive to the noise influence which will result in inconsistent bit string. Although the relating methods of LDP and LTrP explore the distinct information from neighborhoods and Gabor features to make the bit string more stable than the LBP [6], [31]–[33], they still encode the unexpected characteristics in a bit string as similar to the LBP. Consequently, certain effective coding schemes are derived to suppress the noise influence [10], [34]. For instance, the LDN encodes directional information from neighborhoods by using the prominent direction indices (directional numbers) to distinguish the different intensity transitions among the similar structural patterns [10]. The Color Angular Patterns (CAP) of LCVBP calculates the angle values of the referenced pixel and its neighborhoods between a pair of the spectral-band images where the angle values fall between  $0^\circ$  and  $90^\circ$  for extracting discriminative binary patterns [34]. For instance, the angle value at a pixel location between a pair of spectral-band images will be invariant even in the illuminated image region. It indicates that CAP can still encode the illumination invariant binary pattern by using the angle information for color facial images. However, the angle value calculated in CAP is no longer between  $0^\circ$  and  $90^\circ$  for the pairwise directions of vector at a pixel location from grayscale facial images in our LVPs. Therefore, the angle value of the referenced pixel and the neighborhoods encoded by the *threshold function* in CAP might fail in extracting the illumination invariant binary patterns. To remedy this problem, the proposed CST designs the weight vectors of dynamic linear decision function and adopts the sign function to encode the CST value of each neighborhood pixel. Experimental results verify that our coding scheme can suitably suppress the illumination changes and noise influence for encoding more detailed discriminative features than the comparative coding methods.

In our coding scheme, the LVPs generate the binary code by using CST that design the weight vectors of dynamic linear decision function to separate the neighborhoods with the pairwise direction of vector in the 2D distribution. Thus, the basic weight vectors of dynamic linear decision function can be designed as the following form

$$w(G_c) = \left( 1, -\frac{V_{\beta+45^\circ, D}(G_c)}{V_{\beta, D}(G_c)} \right)^T \quad (19)$$

where the first component of weight vectors  $w$  is assigned to “1” that represents the original  $(\beta + 45^\circ)$ -direction value of neighborhood pixel  $G_{p,R}$ , the second component of weight vectors  $w$  which is the transform ratio calculated by using the pairwise direction of vector of the referenced pixel  $G_c$  is used to transform the  $\beta$ -direction value of neighborhood pixel  $G_{p,R}$  to comparative space  $(\beta + 45^\circ)$ -direction.

Therefore, the pairwise direction values of one of the surrounding neighborhoods can be formed as

$$x(G_{p,R}) = (V_{\beta+45^\circ, D}(G_{p,R}), V_{\beta, D}(G_{p,R}))^T \quad (20)$$

where  $x$  called the augmented pattern represents the pairwise direction values of vector of neighborhood pixels  $G_{p,R}$ .

Since the binary code can be considered as a two-class case by using dynamic linear decision function to calculate the CST values of the neighborhoods for encoding a bit string via the sign function, we refer the contexts of  $w$  and  $x$  in (19) and (20) to formulated the dynamic linear decision function as

$$CST(G_{p,R}) = w(G_c)^T \cdot x(G_{p,R}). \quad (21)$$

Consequently, the CST value can be disassembled to (17) as follow

$$\begin{aligned} CST(G_{p,R}) &= w(G_c)^T \cdot x(G_{p,R}) = V_{\beta+45^\circ, D}(G_{p,R}) \\ &\quad - \left( \frac{V_{\beta+45^\circ, D}(G_c)}{V_{\beta, D}(G_c)} \times V_{\beta, D}(G_{p,R}) \right). \end{aligned} \quad (22)$$

Note that the contexts of  $w$ ,  $x$  and  $CST$  can be reformed depending on the pairwise direction values of vector of the referenced pixel and its neighborhoods to dynamic linear decision function for generating the various discriminative features of LVPs.

An example demonstrating the generation of LVP for a given referenced pixel which is marked with red is illustrated in Fig. 3 and Fig. 4. To encode the LVPs,  $LVP_{P,R,\beta}(G_c)$  with pairwise direction of vector  $\beta = 0^\circ$  (marked with red arrow) and  $\beta + 45^\circ = 45^\circ$  (marked with blue arrow) in distance  $D = 1$ , the vectors of the referenced pixel  $G_c$  and its neighborhoods are constructed. The direction values are “4” and “2” in directions  $\beta = 0^\circ$  and  $\beta + 45^\circ = 45^\circ$  at  $G_c$ , respectively. Then, the transform ratio  $V_{\beta+45^\circ, D}(G_c)/V_{\beta, D}(G_c)$  is calculated as “2/4 = 0.5” to transform the  $\beta$ -direction values of the surrounding neighborhoods of  $G_c$  to comparative space  $(\beta + 45^\circ)$ -direction according to the pairwise direction of vector of the referenced pixel  $G_c$ . When we construct the pairwise direction values of vector in directions  $\beta = 0^\circ$  and  $\beta + 45^\circ = 45^\circ$  to the neighborhood pixel “9” marked with yellow, the direction values “-6” and “0” are yielded in directions  $\beta = 0^\circ$  and  $\beta + 45^\circ = 45^\circ$ , respectively. The CST value

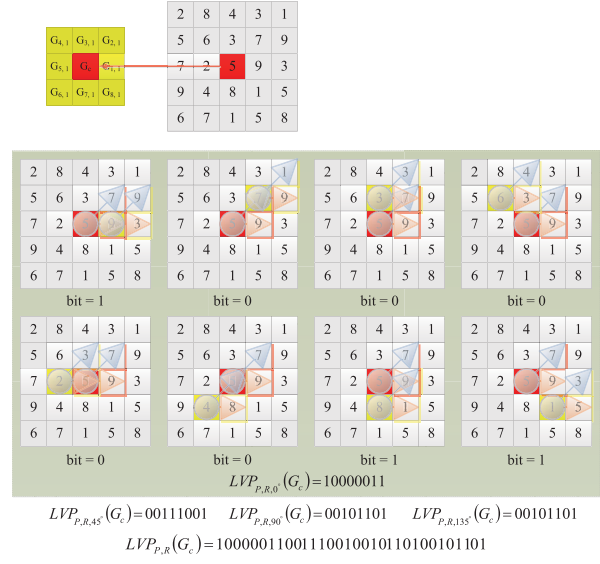


Fig. 4. Example illustrating the encoding of the first-order LVP micropattern.

of the neighborhood pixel “9” is obtained from the difference of original and comparative space  $(\beta + 45^\circ)$ -direction values “0 – (-6 × 0.5) = 3” which is used to encode the first corresponding bit of the 8-bit binary pattern  $LVP_{P,R,0^\circ}(G_c)$  to “1” by using sign function. Similarly, the above procedure is calculated repeatedly with the template in Fig. 1 to generate the complete binary pattern of  $LVP_{P,R,0^\circ}(G_c) = 10000011$  in  $\beta = 0^\circ$  direction of vector with  $D = 1$ . Based on the above scheme, the  $LVP_{P,R,\beta}(G_c)$  in  $\beta = 45^\circ$ ,  $\beta = 90^\circ$  and  $\beta = 135^\circ$  directions of vector are obtained, respectively (three binary patterns of  $LVP_{P,R,45^\circ}(G_c) = 00111001$ ,  $LVP_{P,R,90^\circ}(G_c) = 00101101$  and  $LVP_{P,R,135^\circ}(G_c) = 00101101$  as shown in Fig. 4). Last, the LVP is obtained by concatenating the four binary patterns LVPs as defined in (18) ( $LVP_{P,R}(G_c) = 10000011001110010010110100101101$ ).

Fig. 5 illustrates the visualization of the LBP, second-order LDP, second-order LTrP and the LVP representations that are obtained by applying each of their own descriptors to a referenced image. The visualization of the reconstructed referenced images is created with different grayscale values of circles which provide the variation directions with the values of thermovision scene. It is evident that the micropatterns of these methods show that the LVP extracts more detailed discriminative information than the other local pattern descriptors. Especially, the various pairwise directions of vector provide richer directional information of local texture by using CST. It explains why the proposed LVP can generate more detailed discriminative features and the performance of LVP is more robust than the other comparative methods.

### C. Measurement of Similarity

In [21], the spatial histogram was proposed to model the distribution of LBP for face recognition which provides more robust outcome variations in pose or illumination than existing methods. In this paper, the spatial histogram is also adopted for modeling the distribution of the proposed LVP which extracts

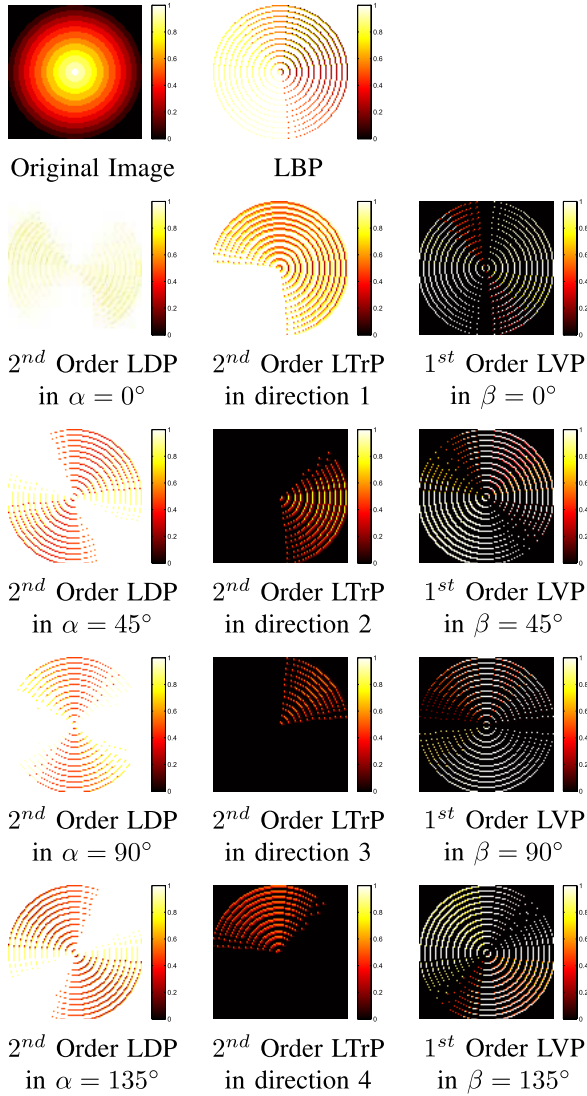


Fig. 5. The applying of LBP, LDP, LTrP, and LVP in generating possible values of binary pattern with each pixel in the original image normalized to 1. The first-order LVP in the zero-order derivative space extracts more additional direction and detailed information than the other descriptors.

discriminative micropatterns via pairwise directions of vector on each pixel in a given local sub-region. In the same way, given an image  $I$  in  $\beta$  direction of vector, the micropatterns of  $LVP_{P,R,\beta}$  are categorized into various parts corresponding to the sub-region  $M_i$  which is denoted by spatially dividing the given image into regular sub-regions  $M_1, \dots, M_L$ , where  $L$  represents the number of sub-regions. Therefore, the spatial histograms  $H_{LVP_{P,R}}(i, \beta)$  can be defined as

$$H_{LVP_{P,R}}(i, \beta) = \{H_{LVP_{P,R,\beta}}(M_i) | i = 1, 2, \dots, L; \beta = 0^\circ, 45^\circ, 90^\circ, 135^\circ\} \quad (23)$$

where  $H_{LVP_{P,R,\beta}}(M_i)$  is the LVP spatial histogram in  $\beta$  direction of vector which is extracted from the local sub-region  $M_i$ , and  $H_{LVP_{P,R}}$  is acquired as the concatenation of the  $H_{LVP_{P,R,\beta}}(M_i)$  for face representation.

The feature vector for the probe image  $U$  represented as  $H_U = \{H_{Ub} | b = 1, 2, \dots, N\}$  is obtained from local pattern descriptor to extract micropatterns into spatial histogram.

Similarly, the feature vector of the gallery image  $V$  in the database can be represented as  $H_V = \{H_{Vb} | b = 1, 2, \dots, N\}$ . The goal is to select the nearest similarity between the probe image and the gallery images. This involves the selection of the best image with nearest similarity measurement between the histograms of the probe image and the gallery images in the database. In order to evaluate the similarity of two histograms, we adopt histogram intersection to measure the two histograms  $H_U$  and  $H_V$ . From formulation, it is defined as

$$S(H_U, H_V) = \sum_{b=1}^N \min(H_{Ub}, H_{Vb}) \quad (24)$$

where  $S(H_U, H_V)$  is the histogram intersection of the two histograms  $H_U$  and  $H_V$ , and  $b$  indicates the index of the total bins  $N$  for each image. As a result, the nearest one (the 1-NN classifier) is the one possessing the minimum value of the histogram intersection between the probe image and the gallery images, which is adopted from (24) to evaluate the performance of the proposed method. Obviously, the common parts of the two histograms can be efficiently calculated with low computational cost.

#### IV. EXTENDING LOCAL VECTOR PATTERN TO HIGH-ORDER DERIVATIVE SPACE

The existing local pattern descriptors, LBP, LDP and LTrP, extract local features using various high-order derivative directions from grayscale images. In our work, the vector of LVP is further refined for extracting more detailed discriminative features in high-order derivative space with the proposed CST coding scheme. It can be observed from the idea of LDP and LTrP that the high-order derivative local patterns are further investigated to extract the feasible and effective 1D direction information of local structure. The original LVP can thereby be conceptually considered as directional non-derivative local pattern descriptor in the zero-order derivative space. Hence, the direction of vector of LVP can be refined in high-order derivative space with variation directions which provides more directional information of local structure than the first-order LVP in the zero-order derivative space. Thereby, the derivative variation direction values obtained from the neighborhoods contribute richer information which can replace the grayscale value to generate the binary code. For example, LDP and LTrP can generate the second-order derivative values in direction  $\alpha = 0^\circ, 45^\circ, 90^\circ$  and  $135^\circ$  [see Fig. 6 (a-1), (b-2), (c-3) and (d-4)] for encoding the third-order LDP and LTrP. Obviously, LDP and LTrP construct the derivative direction values from 1D direction, which can be expanded to 2D direction as the refined vector of second-order LVP in direction  $\alpha = 0^\circ$  and  $\beta = 45^\circ, 90^\circ$  and  $135^\circ$  (for instance, see Fig. 6 (a-2), (a-3) and (a-4)).

When the vector of first-order LVP constructed from  $D = 1$  is implicitly reduced to first-order derivative direction values for encoding the second-order LVP, it only considers 1D direction information. Thus, we develop the second-order LVP adopting both 1D and 2D direction information to refine the directions of vector

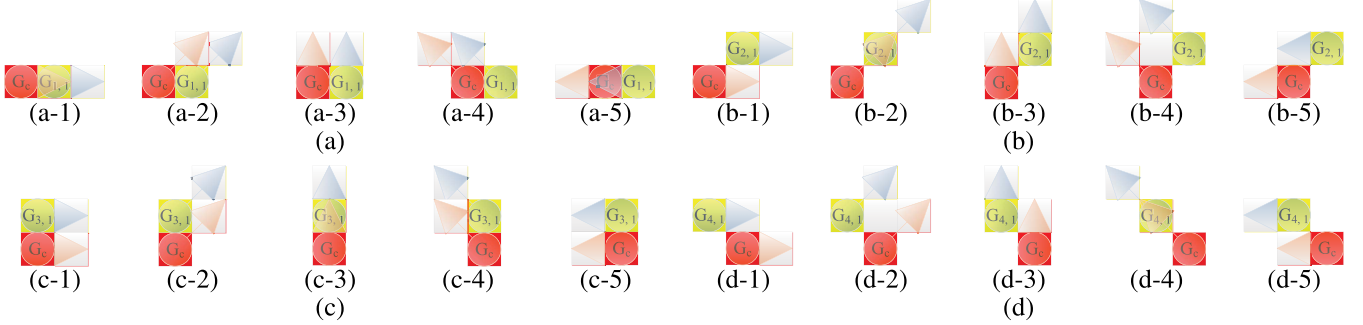


Fig. 6. Illustration of the refined vector of second-order LVP micropattern templates. (a-1) The template for calculating  $\widehat{V}_{\beta=0^\circ, \alpha=0^\circ}(G_c) = V_{\beta=0^\circ, D}(G_{1,R}) - V_{\beta=0^\circ, D}(G_c)$ . (a-2) The template for calculating  $\widehat{V}_{\beta=45^\circ, \alpha=0^\circ}(G_c) = V_{\beta=45^\circ, D}(G_{1,R}) - V_{\beta=45^\circ, D}(G_c)$ . (a-3) The template for calculating  $\widehat{V}_{\beta=90^\circ, \alpha=0^\circ}(G_c) = V_{\beta=90^\circ, D}(G_{1,R}) - V_{\beta=90^\circ, D}(G_c)$ . (a-4) The template for calculating  $\widehat{V}_{\beta=135^\circ, \alpha=0^\circ}(G_c) = V_{\beta=135^\circ, D}(G_{1,R}) - V_{\beta=135^\circ, D}(G_c)$ . (a-5) The template for calculating  $\widehat{V}_{\beta=180^\circ, \alpha=0^\circ}(G_c) = V_{\beta=180^\circ, D}(G_{1,R}) - V_{\beta=180^\circ, D}(G_c)$ . (b-1) The template for calculating  $\widehat{V}_{\beta=0^\circ, \alpha=45^\circ}(G_c) = V_{\beta=0^\circ, D}(G_{2,R}) - V_{\beta=0^\circ, D}(G_c)$ . (b-2) The template for calculating  $\widehat{V}_{\beta=45^\circ, \alpha=45^\circ}(G_c) = V_{\beta=45^\circ, D}(G_{2,R}) - V_{\beta=45^\circ, D}(G_c)$ . (b-3) The template for calculating  $\widehat{V}_{\beta=90^\circ, \alpha=45^\circ}(G_c) = V_{\beta=90^\circ, D}(G_{2,R}) - V_{\beta=90^\circ, D}(G_c)$ . (b-4) The template for calculating  $\widehat{V}_{\beta=135^\circ, \alpha=45^\circ}(G_c) = V_{\beta=135^\circ, D}(G_{2,R}) - V_{\beta=135^\circ, D}(G_c)$ . (b-5) The template for calculating  $\widehat{V}_{\beta=180^\circ, \alpha=45^\circ}(G_c) = V_{\beta=180^\circ, D}(G_{2,R}) - V_{\beta=180^\circ, D}(G_c)$ . (c-1) The template for calculating  $\widehat{V}_{\beta=0^\circ, \alpha=90^\circ}(G_c) = V_{\beta=0^\circ, D}(G_{3,R}) - V_{\beta=0^\circ, D}(G_c)$ . (c-2) The template for calculating  $\widehat{V}_{\beta=45^\circ, \alpha=90^\circ}(G_c) = V_{\beta=45^\circ, D}(G_{3,R}) - V_{\beta=45^\circ, D}(G_c)$ . (c-3) The template for calculating  $\widehat{V}_{\beta=90^\circ, \alpha=90^\circ}(G_c) = V_{\beta=90^\circ, D}(G_{3,R}) - V_{\beta=90^\circ, D}(G_c)$ . (c-4) The template for calculating  $\widehat{V}_{\beta=135^\circ, \alpha=90^\circ}(G_c) = V_{\beta=135^\circ, D}(G_{3,R}) - V_{\beta=135^\circ, D}(G_c)$ . (c-5) The template for calculating  $\widehat{V}_{\beta=180^\circ, \alpha=90^\circ}(G_c) = V_{\beta=180^\circ, D}(G_{3,R}) - V_{\beta=180^\circ, D}(G_c)$ . (d-1) The template for calculating  $\widehat{V}_{\beta=0^\circ, \alpha=135^\circ}(G_c) = V_{\beta=0^\circ, D}(G_{4,R}) - V_{\beta=0^\circ, D}(G_c)$ . (d-2) The template for calculating  $\widehat{V}_{\beta=45^\circ, \alpha=135^\circ}(G_c) = V_{\beta=45^\circ, D}(G_{4,R}) - V_{\beta=45^\circ, D}(G_c)$ . (d-3) The template for calculating  $\widehat{V}_{\beta=90^\circ, \alpha=135^\circ}(G_c) = V_{\beta=90^\circ, D}(G_{4,R}) - V_{\beta=90^\circ, D}(G_c)$ . (d-4) The template for calculating  $\widehat{V}_{\beta=135^\circ, \alpha=135^\circ}(G_c) = V_{\beta=135^\circ, D}(G_{4,R}) - V_{\beta=135^\circ, D}(G_c)$ . (d-5) The template for calculating  $\widehat{V}_{\beta=180^\circ, \alpha=135^\circ}(G_c) = V_{\beta=180^\circ, D}(G_{4,R}) - V_{\beta=180^\circ, D}(G_c)$ . (a)  $\alpha = 0^\circ$ ; (b)  $\alpha = 45^\circ$ ; (c)  $\alpha = 90^\circ$ ; (d)  $\alpha = 135^\circ$ .

for extracting more detailed discriminative features of local patterns in the first-order derivative space.

Given a local sub-region  $I$ , the vector is refined with the first-order derivative along  $0^\circ, 45^\circ, 90^\circ$  and  $135^\circ$  directions being pre-calculated, denoted as  $\widehat{V}_{\beta, \alpha}^1(G_c)$  where  $\alpha = 0^\circ, 45^\circ, 90^\circ, 135^\circ$ , to calculate the second-order LVP in the first-order derivative space as illustrated in Fig. 6 where  $\beta$ -direction of vectors of the referenced pixel and its derivative pixels are marked with red arrow and blue arrow respectively. Moreover, the referenced pixel and its derivative pixels are marked with red and yellow respectively. Let  $G_c$  be a referenced pixel in  $I$ . The four first-order derivative directions of vector at  $G_c$  can be defined as

$$\widehat{V}_{\beta, 0^\circ}^1(G_c) = V_{\beta, D}(G_{1,R}) - V_{\beta, D}(G_c) \quad (25)$$

$$\widehat{V}_{\beta, 45^\circ}^1(G_c) = V_{\beta, D}(G_{2,R}) - V_{\beta, D}(G_c) \quad (26)$$

$$\widehat{V}_{\beta, 90^\circ}^1(G_c) = V_{\beta, D}(G_{3,R}) - V_{\beta, D}(G_c) \quad (27)$$

$$\widehat{V}_{\beta, 135^\circ}^1(G_c) = V_{\beta, D}(G_{4,R}) - V_{\beta, D}(G_c) \quad (28)$$

where  $G_{1,R}, G_{2,R}, G_{3,R}$  and  $G_{4,R}$  are the derivative pixels of the referenced pixel  $G_c$  in  $0^\circ, 45^\circ, 90^\circ$ , and  $135^\circ$  directions, respectively.

In addition, Fig. 6 also illustrates the types of refined direction of vector in second-order LVP templates that can be categorized into 1D direction and 2D direction. Each of the 20 second-order LVP templates can be classified as either 1D direction or 2D direction. For instance, the templates of Fig. 6 (a-1), (a-5), (b-2), (c-3) and (d-4) belong to 1D direction and the remaining templates belong to 2D direction. The operator is also applied to refine the vector of LVP in high-order derivative space.

Then, the second-order LVP in the first-order derivative space,  $LVP_{P,R,\beta,\alpha}^2(G_c)$ , in  $\beta$  direction of vector and  $\alpha$  derivative direction at  $G_c$  is encoded as

$$\begin{aligned} LVP_{P,R,\beta,\alpha}^2(G_c) = & \{ \\ & s_5\left(\widehat{V}_{\beta,\alpha}^1(G_{1,R}), \widehat{V}_{\beta+45^\circ,\alpha}^1(G_{1,R}), \widehat{V}_{\beta,\alpha}^1(G_c), \widehat{V}_{\beta+45^\circ,\alpha}^1(G_c)\right), \\ & s_5\left(\widehat{V}_{\beta,\alpha}^1(G_{2,R}), \widehat{V}_{\beta+45^\circ,\alpha}^1(G_{2,R}), \widehat{V}_{\beta,\alpha}^1(G_c), \widehat{V}_{\beta+45^\circ,\alpha}^1(G_c)\right), \\ & \dots, \\ & s_5\left(\widehat{V}_{\beta,\alpha}^1(G_{p,R}), \widehat{V}_{\beta+45^\circ,\alpha}^1(G_{p,R}), \widehat{V}_{\beta,\alpha}^1(G_c), \widehat{V}_{\beta+45^\circ,\alpha}^1(G_c)\right), \\ & \} |_{p=1,2,\dots,P; R=1} \end{aligned} \quad (29)$$

$$\begin{aligned} & s_5(\widehat{V}_{\beta,\alpha}^1(G_{p,R}), \widehat{V}_{\beta+45^\circ,\alpha}^1(G_{p,R}), \widehat{V}_{\beta,\alpha}^1(G_c), \widehat{V}_{\beta+45^\circ,\alpha}^1(G_c)) \\ & = \begin{cases} 1, & \text{if } \widehat{V}_{\beta+45^\circ,\alpha}^1(G_{p,R}) - \left( \frac{\widehat{V}_{\beta+45^\circ,\alpha}^1(G_c)}{\widehat{V}_{\beta,\alpha}^1(G_c)} \times \widehat{V}_{\beta,\alpha}^1(G_{p,R}) \right) \geq 0 \\ 0, & \text{else} \end{cases} \end{aligned} \quad (30)$$

where  $s_5(\cdot, \cdot)$  is similar to the first-order LVP in the zero-order derivative space, which is used for encoding the relationship between the referenced pixel and its neighborhoods.

Finally, the second-order LVP,  $LVP_{P,R}^2(G_c)$ , at  $G_c$  is defined as the concatenation of the sixteen binary pattern LVPs.

$$LVP_{P,R}^2(G_c) = \{LVP_{P,R,\beta,\alpha}^2(G_c) | \beta = 0^\circ, 45^\circ, 90^\circ, 135^\circ; \alpha = 0^\circ, 45^\circ, 90^\circ, 135^\circ\}. \quad (31)$$

Similar to the second-order LVP in the first-order derivative space, the vectors can be refined with the second-order derivative along  $0^\circ, 45^\circ, 90^\circ$  and  $135^\circ$  directions, denoted as

$\widehat{V}_{\beta,\alpha}^2(G_c)$  where  $\alpha = 0^\circ, 45^\circ, 90^\circ, 135^\circ$ , which is defined as

$$\widehat{V}_{\beta,0^\circ}^2(G_c) = \widehat{V}_{\beta,0^\circ}^1(G_{1,R}) - \widehat{V}_{\beta,0^\circ}^1(G_c) \quad (32)$$

$$\widehat{V}_{\beta,45^\circ}^2(G_c) = \widehat{V}_{\beta,45^\circ}^1(G_{2,R}) - \widehat{V}_{\beta,45^\circ}^1(G_c) \quad (33)$$

$$\widehat{V}_{\beta,90^\circ}^2(G_c) = \widehat{V}_{\beta,90^\circ}^1(G_{3,R}) - \widehat{V}_{\beta,90^\circ}^1(G_c) \quad (34)$$

$$\widehat{V}_{\beta,135^\circ}^2(G_c) = \widehat{V}_{\beta,135^\circ}^1(G_{4,R}) - \widehat{V}_{\beta,135^\circ}^1(G_c). \quad (35)$$

Therefore, the third-order LVP in the second-order derivative space,  $LVP_{P,R,\beta,\alpha}^3(G_c)$ , in  $\beta$  direction of vector and  $\alpha$  derivative direction at  $G_c$  is encoded as

$$\begin{aligned} LVP_{P,R,\beta,\alpha}^3(G_c) = & \{ \\ & s_5(\widehat{V}_{\beta,\alpha}^2(G_{1,R}), \widehat{V}_{\beta+45^\circ,\alpha}^2(G_{1,R}), \widehat{V}_{\beta,\alpha}^2(G_c), \widehat{V}_{\beta+45^\circ,\alpha}^2(G_c)), \\ & s_5(\widehat{V}_{\beta,\alpha}^2(G_{2,R}), \widehat{V}_{\beta+45^\circ,\alpha}^2(G_{2,R}), \widehat{V}_{\beta,\alpha}^2(G_c), \widehat{V}_{\beta+45^\circ,\alpha}^2(G_c)), \\ & \dots, \\ & s_5(\widehat{V}_{\beta,\alpha}^2(G_{p,R}), \widehat{V}_{\beta+45^\circ,\alpha}^2(G_{p,R}), \widehat{V}_{\beta,\alpha}^2(G_c), \widehat{V}_{\beta+45^\circ,\alpha}^2(G_c)), \\ & \}|_{p=1,2,\dots,P; R=1}. \end{aligned} \quad (36)$$

In a general formulation, the  $n^{th}$ -order LVP in the  $(n-1)^{th}$ -order derivative space can be defined by refining the vector with the  $(n-1)^{th}$ -order derivative along  $0^\circ, 45^\circ, 90^\circ$  and  $135^\circ$  directions as

$$\begin{aligned} LVP_{P,R,\beta,\alpha}^n(G_c) = & \{ \\ & s_5(\widehat{V}_{\beta,\alpha}^{n-1}(G_{1,R}), \widehat{V}_{\beta+45^\circ,\alpha}^{n-1}(G_{1,R}), \widehat{V}_{\beta,\alpha}^{n-1}(G_c), \widehat{V}_{\beta+45^\circ,\alpha}^{n-1}(G_c)), \\ & s_5(\widehat{V}_{\beta,\alpha}^{n-1}(G_{2,R}), \widehat{V}_{\beta+45^\circ,\alpha}^{n-1}(G_{2,R}), \widehat{V}_{\beta,\alpha}^{n-1}(G_c), \widehat{V}_{\beta+45^\circ,\alpha}^{n-1}(G_c)), \\ & \dots, \\ & s_5(\widehat{V}_{\beta,\alpha}^{n-1}(G_{p,R}), \widehat{V}_{\beta+45^\circ,\alpha}^{n-1}(G_{p,R}), \widehat{V}_{\beta,\alpha}^{n-1}(G_c), \widehat{V}_{\beta+45^\circ,\alpha}^{n-1}(G_c)), \\ & \}|_{p=1,2,\dots,P; R=1} \end{aligned} \quad (37)$$

where  $\widehat{V}_{\beta,\alpha}^{n-1}(G_c)$  is the refined vector with the  $(n-1)^{th}$ -order derivative in  $\beta$  direction of vector and  $\alpha$  derivative direction at  $G_c$ .

Therefore,  $s_5(\widehat{V}_{\beta,\alpha}^{n-1}(G_{p,R}), \widehat{V}_{\beta+45^\circ,\alpha}^{n-1}(G_{p,R}), \widehat{V}_{\beta,\alpha}^{n-1}(G_c), \widehat{V}_{\beta+45^\circ,\alpha}^{n-1}(G_c))$ ,  $\widehat{V}_{\beta+45^\circ,\alpha}^{n-1}(G_c)$  is defined in (38) which encodes the derivative vector in the  $(n-1)^{th}$ -order derivative space for generating extra useful information in the local sub-region.

$$\begin{aligned} & s_5(\widehat{V}_{\beta,\alpha}^{n-1}(G_{p,R}), \widehat{V}_{\beta+45^\circ,\alpha}^{n-1}(G_{p,R}), \widehat{V}_{\beta,\alpha}^{n-1}(G_c), \widehat{V}_{\beta+45^\circ,\alpha}^{n-1}(G_c)) \\ & = \begin{cases} 1, & \text{if } \widehat{V}_{\beta+45^\circ,\alpha}^{n-1}(G_{p,R}) - \left( \frac{\widehat{V}_{\beta+45^\circ,\alpha}^{n-1}(G_c)}{\widehat{V}_{\beta,\alpha}^{n-1}(G_c)} \times \widehat{V}_{\beta,\alpha}^{n-1}(G_{p,R}) \right) \geq 0 \\ 0, & \text{else.} \end{cases} \end{aligned} \quad (38)$$

The  $n^{th}$ -order LVP in  $(n-1)^{th}$ -order derivative space is defined as

$$\begin{aligned} LVP_{P,R}^n(G_c) = & \{LVP_{P,R,\beta,\alpha}^n(G_c) | \beta = 0^\circ, 45^\circ, 90^\circ, 135^\circ; \\ & \alpha = 0^\circ, 45^\circ, 90^\circ, 135^\circ\}. \end{aligned} \quad (39)$$

Similar to the first-order LVP in the zero-order derivative space, the spatial histogram of the  $n^{th}$ -order LVP in  $(n-1)^{th}$ -order derivative space  $\widehat{H}_{LVP_{P,R}}(i, \beta, \alpha)$  is defined as

$$\begin{aligned} \widehat{H}_{LVP_{P,R}}(i, \beta, \alpha) = & \{\widehat{H}_{LVP_{P,R,\beta,\alpha}}(M_i) | i = 1, 2, \dots, L; \\ & \beta = 0^\circ, 45^\circ, 90^\circ, 135^\circ; \\ & \alpha = 0^\circ, 45^\circ, 90^\circ, 135^\circ\} \end{aligned} \quad (40)$$

where  $\widehat{H}_{LVP_{P,R,\beta,\alpha}}(i, \beta, \alpha)$  is the high-order LVP spatial histogram in  $\beta$  direction of vector and  $\alpha$  derivative direction which is extracted from the local sub-region  $M_i$ .

The local pattern descriptor LVP in high-order derivative space is capable of generating more detailed discriminative texture information than the first-order LVP. Thus, the second-order LVP encoding both 1D and 2D direction information can achieve better performance than the first-order LVP which only encodes the 1D direction information. In LDP, the 1D high-order derivative direction values lead to the noise which results in the deteriorating of the performance. Especially, the performance of the fourth-order LDP drops significantly by using the 1D third-order derivative direction values. Unfortunately, the proposed LVP encounters the same problem in higher order derivative space. The reasons are: (1) the 1D derivative direction values of high-order LVP is similar to the LDP, (2) the third-order LVP only considers the same derivative direction to refine both 1D and 2D direction information of local texture which leads to the similar problem in (1).

The merits of our proposed LVP comparing with the other local pattern descriptors can be summarized as follows:

- 1) Apparently, the number of the distinct values is decided by using the number of the derivative directions. In general, the feature length increases with exponential growth by using more derivative directions. However, the LVP reduces the feature length better than the LTrP by using the CST with pairwise direction of vector which is used to encode the LVP. It can be observed that the feature length of the LTrP is 12 times of the first-order LVP in zero-order derivative space under single pairwise direction of vector.
- 2) The numbers of distinct values of LBP, LDP, LTrP and LVP are two, two, four and two. Even though the LTrP encodes images with four distinct values where the tetra patterns are encoded based on the quadrant of the referenced pixel, it still leads to the other tetra patterns being encoded with "0" and loses the potential information possibly. In our proposed LVP, it adopts the CST via pairwise directions of vector to extract more feasible detailed discriminative information so as to conquer the high redundancy problem.
- 3) The  $n^{th}$ -order LDP encodes the four binary patterns based on the  $(n-1)^{th}$ -order derivatives along  $0^\circ, 45^\circ, 90^\circ$ , and  $135^\circ$  directions respectively, whereas the  $n^{th}$ -order LVP in the  $(n-1)^{th}$ -order derivative space encodes the sixteen binary patterns based on the four pairwise directions of vector with  $(n-1)^{th}$ -order derivatives along  $0^\circ, 45^\circ, 90^\circ$ , and  $135^\circ$  direction spaces. It indicates that the  $n^{th}$ -order LVP adopts both 1D and 2D direction information to extract the local patterns, whereas the  $n^{th}$ -order LDP only uses 1D direction information. Hence, the  $n^{th}$ -order LVP provides more detailed discriminative features than the  $n^{th}$ -order LDP.

## V. EXPERIMENTAL RESULTS

In this section, we will present various experiments conducted to demonstrate the performance of the proposed and comparative methods. In our experiments, numerous publicly available face databases are used, such as FERET [24], CAS-PEAL [25], CMU-PIE [26], Extended Yale B [27], [28], and LFW [29] databases. The environmental factors considered in these databases include pose, illumination, expression, aging and accessory variations etc. In the following experiments, all the original facial images were normalized and cropped to  $64 \times 64$  except that the Extended Yale B database was normalized to  $96 \times 84$  based on the location of the two eyes. Since the cropped images were normalized to a resolution of  $64 \times 64$ , the experiments were naturally expected to show lower performance than other published results such as [11] where higher resolution was used for the FERET database cropped images. Moreover, each image is partitioned with  $4 \times 4$  sub-regions and uses the uniform quantization method to reduce the number of histogram bins in each sub-region from 256 to 8. Experiment A reports the experimental results on the FERET database with illumination, expression and aging variations. Our experimental environment replicates the research of Zhang *et al.* with the similar parameters setting and noise influence for evaluating the comparative performances [22]. Experiment B illustrates the experimental results on the CAS-PEAL database with expression, lighting, accessory, background, distance and aging variations. Experiment C reports the experimental results on the CMU-PIE database with pose, illumination and expression variations. Experiment D provides the experimental results on the Extended Yale B database with severe illumination variations. Experiment E reports the experimental results on the LFW database with pose, illumination and expression variations. Furthermore, the Gabor features are investigated to provide more feasible and effective feature images and then used for object recognition the same as other methods do [31], [35], [36]. For comparison purpose, the LBP, LDP, LTrP and the proposed LVP methods also use the Gabor features to evaluate the effectiveness for face recognition. In order to distinguish the use of Gabor features with eight orientations of the kernel, the methods mentioned above are renamed as GLBP, GLDP, GLTrP and GLVP. Additionally, all the experiments were conducted to compare the proposed LVP in high-order derivative space with the LBP, LDP, and LTrP with input grayscale images and evaluate the effectiveness of GLBP, GLDP, GLTrP and GLVP with Gabor features. Table I tabulates the abbreviations and descriptions of the proposed and comparative methods as denoted in the analysis of experimental results.

### A. Experimental Results on FERET Database

In this experiment, the FERET [24] face database is used to evaluate the comparative experiments between the proposed LVP and the other methods for face recognition. The FERET database provides the evaluation protocol as gallery (*Fa*) and probe sets (*Fb*, *Fc*, *Dup I* and *Dup II*) that are used to evaluate the performance of the above methods. The gallery set in *Fa* consists of 1,196 frontal facial images of 1,196 subjects,

TABLE I  
THE ABBREVIATIONS AND DESCRIPTIONS OF THE PROPOSED AND COMPARATIVE METHODS

Abbreviation	Description
<i>LBP</i>	Local Binary Pattern encodes the binary pattern by comparing the referenced pixel and its neighborhoods.
<i>GLBP</i>	Extending LBP to Gabor features.
<i>LDP</i>	Derived from LBP, Local Derivative Pattern encodes the turning points or the monotonical ones to the two distinct values ("1" or "0") by comparing the derivative values between the referenced pixel and its local neighborhoods in a given single high-order derivative direction.
<i>GLDP</i>	Extending LDP to Gabor features.
<i>LTrP</i>	Different from LDP, Local Tetra Pattern extends the two distinct values to four distinct values by using quadrants of the referenced pixel and surrounding neighbors which are calculated from both the horizontal and vertical high-order derivative values.
<i>GLTrP</i>	Extending LTrP to Gabor features.
<i>LVP</i>	Derived from LTrP, Local Vector Pattern proposes a novelty vector representation which is encoded by the proposed CST via dynamic linear decision function and various pairwise directions of vector of the referenced pixel and its neighborhoods in high-order derivative space in an attempt to generating the complete binary code of micropatterns.
<i>GLVP</i>	Extending LVP to Gabor features.

the probe set in *Fb* consists of 1,195 images with various expression conditions, the probe set in *Fc* consists of 194 images with different illumination conditions, the probe set in *Dup I* consists of 722 images captured in time between one minute and 1,031 days, and the probe set in *Dup II* consists of 234 images which is a strict subset of *Dup I* captured only at least after 18 months. In addition, we also conduct the four probe sets to obtain the average recognition rate of the proposed and comparative methods. For each probe image, the framework selects the nearest image by measuring the similarity computed using (24). If the selected gallery image belongs to the same category as the probe image, it means that the framework finds the expected image. Otherwise, the framework fails in finding an appropriate image.

The LVP first generates a complete binary code of micropatterns by using various pairwise directions of vector which is computed based on the parameter *D*. Then, we test the parameter *D* to evaluate the performance of the proposed method. Experimental results illustrated in Fig. 7(e) demonstrates that the average recognition rate is significantly affected by parameter *D*. In LVP, the performance drops when parameter *D* = 3 in different orders of derivative space with grayscale images and Gabor features respectively. It is due to the fact that the correlation of vector decreases when the value of parameter *D* increases. Moreover, the LVP exhibits better performance than the other methods even under the same order derivative space. To be more precise, the LVP can extract more detailed discriminative information than the other comparative methods with grayscale images and Gabor features respectively.

In order to discuss the selections of parameter setting in affecting the performance of the various methods, the sub-region size and the number of histogram bins are varied and the experiments are conducted on the grayscale images again as shown in Fig. 8. The varying sub-region sizes,  $4 \times 4$ ,  $8 \times 8$

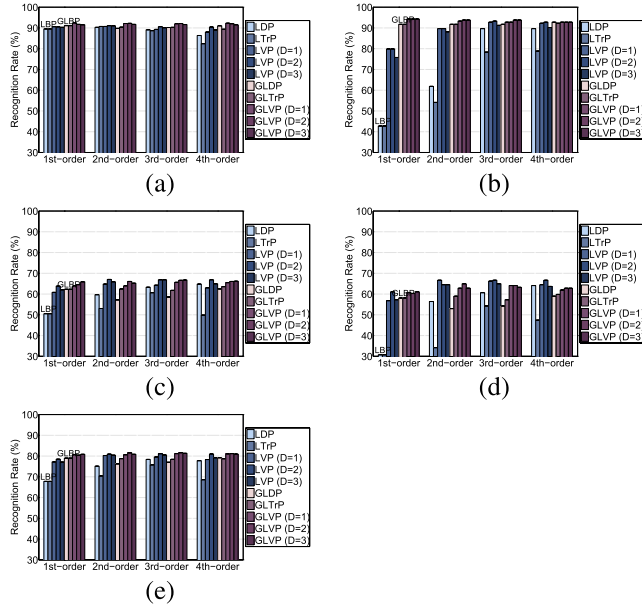


Fig. 7. Comparative recognition accuracies between different orders of LBP/GLBP, LDP/GLDP, LTrP/GLTrP and LVP/GLVP on the FERET data sets. (a) Result conducting on *Fb*, (b) result conducting on *Fc*, (c) result conducting on *Dup I*, (d) result conducting on *Dup II*, (e) average recognition result.

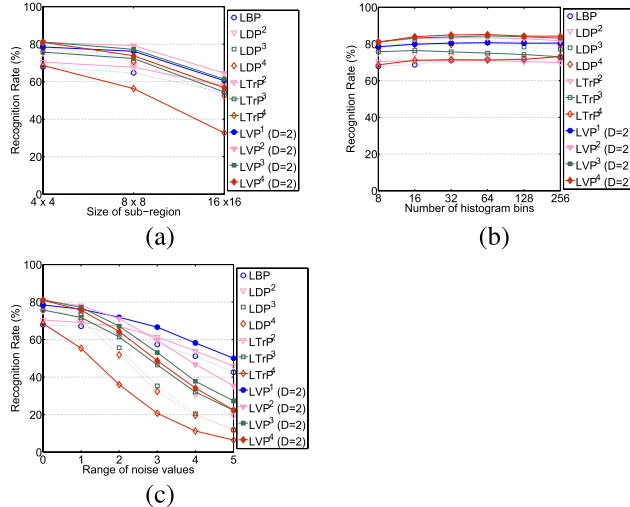


Fig. 8. Comparative recognition accuracies of the LBP/GLBP, LDP/GLDP, LTrP/GLTrP and LVP/GLVP on the FERET database with (a) different sub-region sizes, (b) different histogram bins, and (c) different range of noise values added to the probe images.

and  $16 \times 16$  are tested with the fixed 8 histogram bins in each sub-region and the average recognition rate is summarized in Fig. 8(a). It reveals that the performance drops due to the increasing sub-region size that influences the feature extraction in spatial information. To test the varying histogram bins, 8, 16, 32, 64, 128 and 256 with the fixed  $4 \times 4$  sized sub-region, the uniform quantization method is adopted to partition the spatial histogram into equal interval. All the proposed and comparative methods exhibit flat curves in average recognition rate as shown in Fig. 8(b). It conveys that the feature length can be effectively reduced to 8 histogram bins. As a result,

TABLE II  
FEATURE LENGTH OF PROBE IMAGE USING VARIOUS METHODS

Methods	Feature Length
<i>LBP</i>	8
<i>GLBP</i>	$8 \times 8$
<i>LDP</i>	$8 \times 4$
<i>GLDP</i>	$8 \times 8 \times 4$
<i>LTrP</i>	$8 \times 13$
<i>GLTrP</i>	$8 \times 8 \times 13$
<i>LVP<sup>1</sup>(D = 1, 2, 3)</i>	$8 \times 4$
<i>LVP<sup>n</sup>(D = 1, 2, 3)</i>	$8 \times 16$
<i>GLVP<sup>1</sup>(D = 1, 2, 3)</i>	$8 \times 8 \times 4$
<i>GLVP<sup>n</sup>(D = 1, 2, 3)</i>	$8 \times 8 \times 16$

the LVP performs much better than the comparative methods under various testing parameters according to the experimental results in both Fig. 8(a) and Fig. 8(b).

One of the issues for local texture extraction is that the local pattern descriptors are sensitive to noise. Hence, a noisy influence experiment for the proposed and the other comparative methods is investigated. The parameters remain unchanged in the same FERET database except that all the images in the probe sets are reconstructed by adding the random noise with different range of values. The experimental results as shown in Fig. 8(c) demonstrate that the first-order LVP using the proposed CST can effectively suppress the slight noise influence which performs much better than the comparative methods in high-order derivative space. Moreover, the recognition accuracies of all these methods drop in the high-order derivative spaces due to the fact that the noise will be generated from the high-order derivative values.

Table II tabulates the feature length for a sub-region in a given image by using LBP, LDP, LTrP and LVP with grayscale images and Gabor features. The feature length of the first-order LVP is 4 times of the LBP, and the feature length of the LVP is 4 and 16/13 times of the LDP and the LTrP in high-order derivative space respectively. Although the feature length of the LVP is slightly higher, the performance is significantly improved in terms of average recognition rate comparing with the other methods. Fig. 7(e) illustrates the average recognition rates of all these methods. From Fig. 7, we can observe that: (1) The first-order LVP outperforms the LBP by 10.7% and the first-order GLVP outperforms the GLBP by 1.41%; (2) In the first-order derivative space, the LVP performs better than the LDP by 5.8% and the LTrP by 10.49%, and the GLVP outperforms the GLDP by 5.33% and the GLTrP by 2.81%; (3) In the second-order derivative space, the LVP works better than the LDP by 2.77% and the LTrP by 5.37%, and the GLVP outperforms the GLDP by 4.61% and the GLTrP by 3.2%; (4) In the third-order derivative space, the performance of LVP is enhanced 3.24% comparing with the LDP and the LTrP by 12.41%, and the GLVP outperforms the GLDP by 2% and the GLTrP by 2.47%. In addition, we can find that both LVP and GLVP still achieves the best recognition rate among all methods on the four probe sets (*Fb*, *Fc*, *Dup I* and *Dup II*) as shown in Fig. 7. Hence, these results further demonstrate the stable performance of both LVP and GLVP for face recognition.

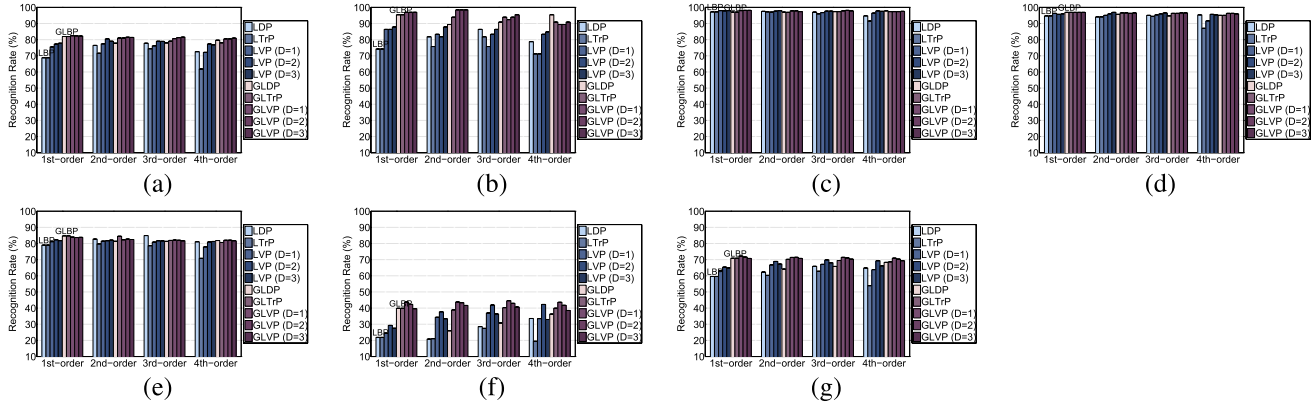


Fig. 9. Comparative recognition accuracies between different orders of LBP/GLBP, LDP/GLDP, LTrP/GLTrP and LVP/GLVP on the CAS-PEAL data sets. (a) Result conducting on *Acc.*, (b) result conducting on *Age*, (c) result conducting on *Back.*, (d) result conducting on *Dist.*, (e) result conducting on *Expr.*, (f) result conducting on *Light.*, (g) average recognition result.

TABLE III  
FEATURE EXTRACTION AND MATCHING TIME (SECONDS) OF  
COMPARATIVE METHODS ON FERET DATABASE

Method	Feature extraction	Feature matching
<i>LBP</i>	279.51	31.26
<i>LDP</i> <sup>2</sup>	316.42	83.90
<i>LDP</i> <sup>3</sup>	303.83	85.68
<i>LDP</i> <sup>4</sup>	292.64	84.30
<i>LTrP</i> <sup>2</sup>	971.01	248.01
<i>LTrP</i> <sup>3</sup>	922.76	252.72
<i>LTrP</i> <sup>4</sup>	876.51	249.68
<i>LVP</i> <sup>1</sup> ( <i>D</i> = 1)	351.28	85.69
<i>LVP</i> <sup>2</sup> ( <i>D</i> = 1)	1962.73	300.05
<i>LVP</i> <sup>3</sup> ( <i>D</i> = 1)	1855.88	305.09
<i>LVP</i> <sup>4</sup> ( <i>D</i> = 1)	1739.13	305.65
<i>LVP</i> <sup>1</sup> ( <i>D</i> = 2)	328.07	86.56
<i>LVP</i> <sup>2</sup> ( <i>D</i> = 2)	1831.20	304.56
<i>LVP</i> <sup>3</sup> ( <i>D</i> = 2)	1737.04	312.49
<i>LVP</i> <sup>4</sup> ( <i>D</i> = 2)	1604.91	306.25
<i>LVP</i> <sup>1</sup> ( <i>D</i> = 3)	313.08	84.91
<i>LVP</i> <sup>2</sup> ( <i>D</i> = 3)	1741.16	298.96
<i>LVP</i> <sup>3</sup> ( <i>D</i> = 3)	1619.32	306.99
<i>LVP</i> <sup>4</sup> ( <i>D</i> = 3)	1510.74	307.06

We also compared the computation time of all methods on the FERET database. Table III lists the feature extraction and feature matching time of all methods. It is reasonable that our method needs to spend more time on feature extraction and feature matching in high-order derivative space for generating more detailed discriminative features than the other methods. We can observe that plenty of boundary pixels are ignored in extracting the features so that the feature extraction time of LVP will decrease when the parameter *D* increases. It can be considered as a trade-off between computation cost and performance with parameter *D*. The experimental results demonstrate that the proposed LVP delivers the best performance when parameter *D* = 2.

#### B. Experimental Results on CAS-PEAL Database

The CAS-PEAL [25] face database is also used to evaluate the performance of the proposed LVP with the other methods. The database contains 9,060 images of 1,040 subjects. In the

CAS-PEAL standard subset, the gallery set contains 1,040 frontal images, the *Acc.* probe set contains 2,046 accessory images, the *Age* probe set contains 66 aging images, the *Back.* probe set contains 650 background images, the *Dist.* probe set contains 324 distance images, the *Expr.* probe set contains 1,884 expression images, and the *Light.* probe set contains 2,450 lighting images.

The experimental results illustrated in Fig. 9 demonstrate that the recognition accuracy is improved by using the proposed LVP to extract more detailed information than the other existing methods. Moreover, we test all methods on the Gabor features for enhancing the performance of each method on the grayscale images. The results illustrate that Gabor features can provide more detailed discriminative information than grayscale images. For instance, 9(f) illustrates that the performance of face recognition is significantly improved in different orders of derivative spaces and hence verify that the proposed CST can effectively suppress the lighting changes. Simply speaking, both LVP and GLVP achieve best recognition accuracy than the other methods as demonstrated in Fig. 9.

#### C. Experimental Results on CMU-PIE Database

The CMU-PIE [26] database is used to test and evaluate the performances between the proposed LVP and the other methods under extensive variations of pose, illumination, and expression. The database contains 11,560 facial images of 68 subjects where each subject consists of 170 facial images. In the experiments, the images randomly selected from each subject in the database are used as the gallery set and the others as the probe set. Hence, the four gallery sets contain images of 1, 3, 6 and 9 from each subject, respectively. For each gallery set, we perform test runs of 170, 56, 28 and 18 for each method to generate the average recognition rate and standard deviation as illustrated in Fig. 10. It is evident that the average recognition rates increase depending on the variation of gallery set sizes. From Fig. 10, the proposed LVP and GLVP outperform the other methods among all the comparative results. More specifically, LVP is significantly better than the other methods when the gallery set size is small. For instance, (1) the first-order LVP outperforms the LBP by

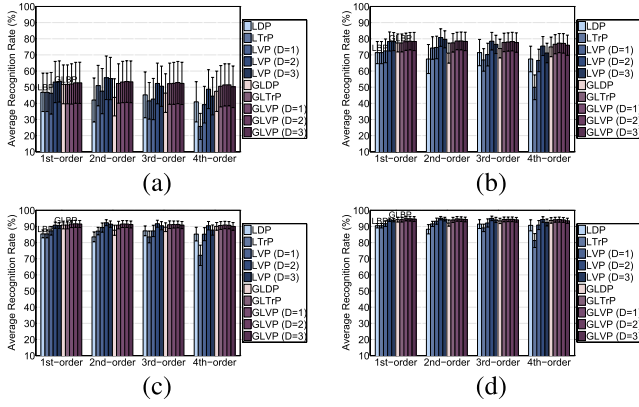


Fig. 10. Comparative average recognition accuracies between different orders of LBP/GLBP, LDP/GLDP, LTrP/GLTrP and LVP/GLVP on the CMU-PIE database. (a) Result conducting on the first gallery set (one image from each subject), (b) result conducting on the second gallery set (three images from each subject), (c) result conducting on the third gallery set (six images from each subject), (d) result conducting on the fourth gallery set (nine images from each subject).

6.36%, (2) In the first-order derivative space, the performance of LVP is increased by 13.77% comparing with the LDP and 4.86% comparing with the LTrP, (3) In the second-order derivative space, the LVP outperforms the LDP by 7.06% and the LTrP by 10.77%, (4) In the third-order derivative space, the LVP outperforms the LDP by 7.83% and the LTrP by 23.08% when the gallery set size is 1. Conclusively, these results demonstrate that both LVP and GLVP work better than the other methods under variation conditions. We can notice that the LVP delivers the best performance in face recognition when parameter  $D = 2$  which demonstrates that the correlation of vector decreases when the value of parameter  $D$  increases.

#### D. Experimental Results on Extended Yale B Database

Here, the Extended Yale B face database is used to demonstrate the comparative performances between the proposed LVP and the other methods under severe illumination variations. The experimental database contains 2,432 frontal facial images of 38 subjects with 64 different illumination variations. All the facial images have been aligned and cropped to  $192 \times 168$  pixels from the database websites. To evaluate the performance with the same parameter settings as in the previous experiments, these facial images are normalized to  $96 \times 84$  pixels. Each image from the subject in the database is used as the gallery set and the others as the probe set. Then, we perform 64 run of tests for each method with 1-NN classifier. The experimental results reporting the comparative average recognition rates and standard deviations of the LVP, GLVP and the other methods are illustrated in Fig. 11. Apparently, the LVP significantly improves the performance of face recognition than the other methods even under severe illumination variations.

#### E. Experimental Results on LFW Database

Additionally, we also test the LFW [29] database which contains 13,233 face images from 5,749 different individuals.

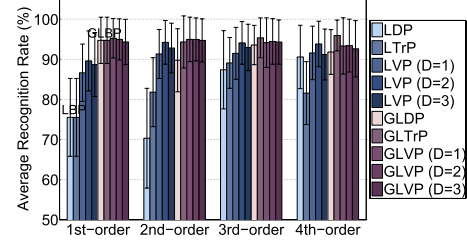


Fig. 11. Comparative average recognition accuracies between the different orders of LBP/GLBP, LDP/GLDP, LTrP/GLTrP and LVP/GLVP on the Extended Yale B database.

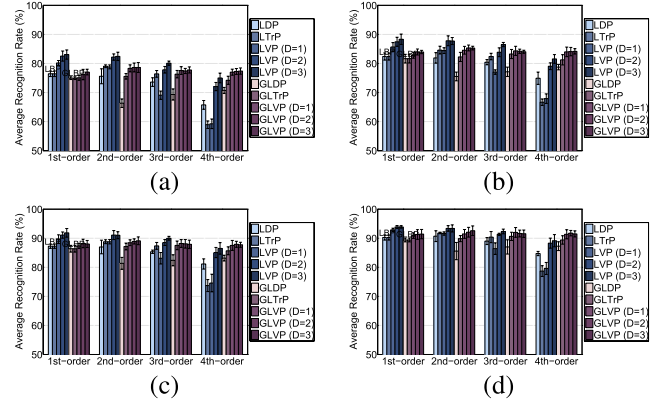


Fig. 12. Comparative average recognition accuracies between different orders of LBP/GLBP, LDP/GLDP, LTrP/GLTrP and LVP/GLVP on the LFW database. (a) Result conducting on *Sub 1* (number of images for each person is larger than 20), (b) result conducting on *Sub 2* (number of images for each person is larger than 30), (c) result conducting on *Sub 3* (number of images for each person is larger than 40), (d) result conducting on *Sub 4* (number of images for each person is larger than 50).

The LFW experiments were conducted only on the 1,680 people who have two or more than two face images and ignored the remained 4,069 people who have just one image. These images are captured from the real world including various conditions of facial expression, illuminations, pose and occlusions. Here, we use the aligned version of images [37] from the database website which are categorized into four subsets based on the number of images for each person. The four subsets are: *Sub 1* (number of images for each person is larger than 20), *Sub 2* (number of images for each person is larger than 30), *Sub 3* (number of images for each person is larger than 40) and *Sub 4* (number of images for each person is larger than 50). We carry out a 5-fold cross-validation scheme where each subset is randomly partitioned into five groups. The four groups are used as the gallery set and the remaining group is used as the probe set. The above process is repeated five times to calculate the average recognition rate.

In the experiment, we test the proposed method and compare it with the state-of-the-art local pattern descriptors, such as LBP, LDP, LTrP, LDIP, LDN and LCVBP for face recognition. The LDIP [6] and LDN [10] also try to use Gabor features for enhancing the recognition accuracy and these methods are renamed as GLDiP and GLDN. For LCVBP [34], we use  $RQCr$  ( $R$  taken from  $RGB$ ,  $Q$  taken from  $YIQ$ , and  $C_r$  taken from  $YCbCr$ ) color representation to encode the complete

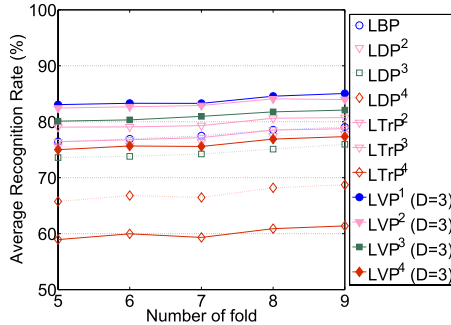


Fig. 13. Comparative average recognition accuracies with multi-fold cross-validation of the LBP, LDP, LTrP and LVP( $D=3$ ) on the Sub 1.

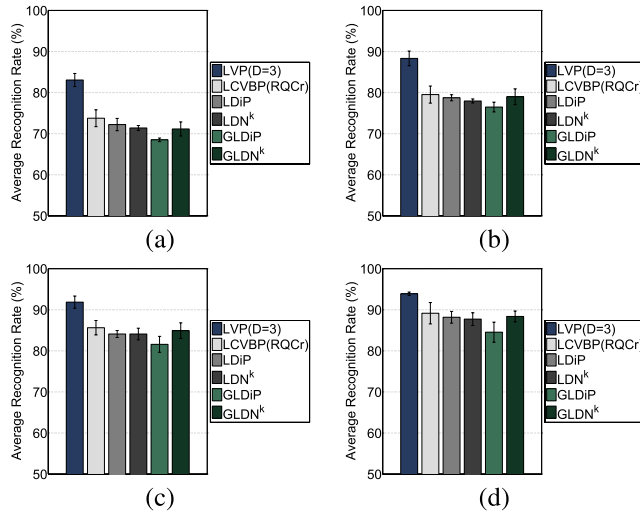


Fig. 14. Comparative average recognition accuracies of LVP, LCVBP, LDIP/GLDiP and LDN/GLDN on the LFW database. (a) Result conducting on Sub 1 (number of images for each person is larger than 20), (b) result conducting on Sub 2 (number of images for each person is larger than 30), (c) result conducting on Sub 3 (number of images for each person is larger than 40), (d) result conducting on Sub 4 (number of images for each person is larger than 50).

binary code. For LDN [10], we use the Kirsch compass masks to generate the edge responses of neighborhoods for encoding the complete binary code. Fig. 12 reports the average recognition rate and standard deviation of each method and it is evident that both LVP and GLVP outperform the other methods on the four subsets (*Sub 1*, *Sub 2*, *Sub 3*, *Sub 4*). In addition, we also test multi-fold cross-validation in *Sub 1* to evaluate the stability of performance in our proposed LVP ( $D = 3$ ) and competing methods as illustrated in Fig. 13. The results demonstrate that the proposed LVP works better than the other methods in different orders derivative spaces. In addition, our best recognition result is compared with LDIP/GLDiP, LDN/GLDN and LCVBP as shown in Fig. 14. These experimental results demonstrate the effectiveness of our proposed LVP in real-word applications.

## VI. CONCLUSIONS AND FUTURE WORK

In this paper, a novel local pattern descriptor, Local Vector Pattern (LVP), is devised and investigated for generating effective and powerful representation for use in face recognition.

First of all, we develop a novel vector representation by calculating the various directions with diverse distances to represent the 1D direction and structure information of the face texture. Based on the vector representation, the LVP encodes various pairwise directions of vector as a facial descriptor to strengthen the structure of micropatterns. Moreover, a novel coding scheme, Comparative Space Transform (CST), in LVP encoding is proposed to encode a pairwise direction of vector for reducing the feature length and high redundancy resulting from LTrP. Furthermore, the proposed CST that uses a designed dynamic linear decision function can suppress the slight noise influence, such as intensity change in a flat surface. The proposed LVP can also be applied in various high-order derivative spaces to refine the vector representation for obtaining a more compact and discriminative local pattern descriptor. Last, the measurement of similarity that performs histogram intersection is adopted to evaluate the performance with several public face databases such as FERET, CAS-PEAL, CMU-PIE, Extended Yale B and LFW databases. Experimental results demonstrate that the proposed method outperforms several state-of-the-art local pattern descriptors in face recognition.

In the literature, the directional information from neighborhoods was discussed by using a compass mask, such as the derivative-Gaussian mask which was developed to tolerate noise and illumination variation for generating the edge responses in various directions. In the future, the stable direction information of local structure will be explored for extracting more distinctive features by combining the proposed CST coding scheme to further improve the performance. Meanwhile, it can be expected that the proposed method can also work well in other pattern recognition applications, such as object recognition, gender recognition, and so on, because of the inherent characteristic of robustness in extracting discriminative features.

## REFERENCES

- [1] X. Xie and K.-M. Lam, "Gabor-based kernel PCA with doubly nonlinear mapping for face recognition with a single face image," *IEEE Trans. Image Process.*, vol. 15, no. 9, pp. 2481–2492, Sep. 2006.
- [2] X. Chai, S. Shan, X. Chen, and W. Gao, "Locally linear regression for pose-invariant face recognition," *IEEE Trans. Image Process.*, vol. 16, no. 7, pp. 1716–1725, Jul. 2007.
- [3] W.-P. Choi, S.-H. Tse, K.-W. Wong, and K.-M. Lam, "Simplified Gabor wavelets for human face recognition," *Pattern Recognit.*, vol. 41, no. 3, pp. 1186–1199, Mar. 2008.
- [4] J. Y. Choi, K. N. Plataniotis, and Y. M. Ro, "Face feature weighted fusion based on fuzzy membership degree for video face recognition," *IEEE Trans. Syst., Man, Cybern. B, Cybern.*, vol. 42, no. 4, pp. 1270–1282, Aug. 2012.
- [5] W. Zhao, R. Chellappa, P. J. Phillips, and A. Rosenfeld, "Face recognition: A literature survey," *ACM Comput. Surv.*, vol. 35, no. 4, pp. 399–459, 2003.
- [6] T. Jabid, M. H. Kabir, and O. Chae, "Local directional pattern (LDP) for face recognition," in *Proc. IEEE Int. Conf. Consum. Electron.*, Mar. 2010, pp. 329–330.
- [7] J. Y. Choi, Y. M. Ro, and K. N. Plataniotis, "A comparative study of preprocessing mismatch effects in color image based face recognition," *Pattern Recognit.*, vol. 44, no. 2, pp. 412–430, 2011.
- [8] J. Y. Choi, Y. M. Ro, and K. N. Plataniotis, "Boosting color feature selection for color face recognition," *IEEE Trans. Image Process.*, vol. 20, no. 5, pp. 1425–1434, May 2011.
- [9] J. Y. Choi, Y. M. Ro, and K. N. Plataniotis, "Color local texture features for color face recognition," *IEEE Trans. Image Process.*, vol. 21, no. 3, pp. 1366–1380, Mar. 2012.

- [10] R. Rivera, J. R. Castillo, and O. Chae, "Local directional number pattern for face analysis: Face and expression recognition," *IEEE Trans. Image Process.*, vol. 22, no. 5, pp. 1740–1752, May 2013.
- [11] M. Yang, L. Zhang, S. C. K. Shiu, and D. Zhang, "Monogenic binary coding: An efficient local feature extraction approach to face recognition," *IEEE Trans. Inf. Forensics Security*, vol. 7, no. 6, pp. 1738–1751, Dec. 2012.
- [12] M. Turk and A. Pentland, "Eigenfaces for recognition," *J. Cognit. Neurosci.*, vol. 3, no. 1, pp. 71–86, 1991.
- [13] P. N. Belhumeur, J. P. Hespanha, and D. J. Kriegman, "Eigenfaces vs. Fisherfaces: Recognition using class specific linear projection," *IEEE Trans. Pattern Anal. Mach. Intell.*, vol. 19, no. 7, pp. 711–720, Jul. 1997.
- [14] X. He, S. Yan, Y. Ho, P. Niyogi, and H. J. Zhang, "Face recognition using Laplacianfaces," *IEEE Trans. Pattern Anal. Mach. Intell.*, vol. 27, no. 3, pp. 328–340, Mar. 2005.
- [15] D. Cai, X. He, J. Han, and H. Zhang, "Orthogonal Laplacianfaces for face recognition," *IEEE Trans. Image Process.*, vol. 15, no. 11, pp. 3608–3614, Nov. 2006.
- [16] S. Yan, D. Xu, B. Zhang, H. J. Zhang, Q. Yang, and S. Lin, "Graph embedding and extensions: A general framework for dimensionality reduction," *IEEE Trans. Pattern Anal. Mach. Intell.*, vol. 29, no. 1, pp. 40–51, Jan. 2007.
- [17] H. F. Hu, "Orthogonal neighborhood preserving discriminant analysis for face recognition," *Pattern Recognit.*, vol. 41, no. 6, pp. 2045–2054, 2008.
- [18] T. Ojala, M. Pietikäinen, and D. Harwood, "A comparative study of texture measures with classification based on feature distributions," *Pattern Recognit.*, vol. 29, no. 1, pp. 51–59, 1996.
- [19] M. Pietikäinen, T. Ojala, and Z. Xu, "Rotation-invariant texture classification using feature distributions," *Pattern Recognit.*, vol. 33, no. 1, pp. 43–52, 2000.
- [20] T. Ojala, M. Pietikäinen, and T. Mäenpää, "Multiresolution gray-scale and rotation invariant texture classification with local binary patterns," *IEEE Trans. Pattern Anal. Mach. Intell.*, vol. 24, no. 7, pp. 971–987, Jul. 2002.
- [21] T. Ahonen, A. Hadid, and M. Pietikäinen, "Face description with local binary patterns: Application to face recognition," *IEEE Trans. Pattern Anal. Mach. Intell.*, vol. 28, no. 12, pp. 2037–2041, Dec. 2006.
- [22] B. Zhang, Y. Gao, S. Zhao, and J. Liu, "Local derivative pattern versus local binary pattern: Face recognition with higher-order local pattern descriptor," *IEEE Trans. Image Process.*, vol. 19, no. 2, pp. 533–544, Feb. 2010.
- [23] S. Murala, R. P. Maheshwari, and R. Balasubramanian, "Local tetra patterns: A new feature descriptor for content-based image retrieval," *IEEE Trans. Image Process.*, vol. 21, no. 5, pp. 2874–2886, May 2012.
- [24] P. J. Phillips, H. Moon, S. A. Rizvi, and P. J. Rauss, "The FERET evaluation methodology for face-recognition algorithms," *IEEE Trans. Pattern Anal. Mach. Intell.*, vol. 22, no. 10, pp. 1090–1104, Oct. 2000.
- [25] W. Gao *et al.*, "The CAS-PEAL large-scale Chinese face database and baseline evaluations," *IEEE Trans. Syst., Man, Cybern. A, Syst., Humans*, vol. 38, no. 1, pp. 149–161, Jan. 2008.
- [26] T. Sim, S. Baker, and M. Bsat, "The CMU pose, illumination, and expression database," *IEEE Trans. Pattern Anal. Mach. Intell.*, vol. 25, no. 12, pp. 1615–1618, Dec. 2003.
- [27] A. S. Georghiades, P. N. Belhumeur, and D. J. Kriegman, "From few to many: Illumination cone models for face recognition under variable lighting and pose," *IEEE Trans. Pattern Anal. Mach. Intell.*, vol. 23, no. 6, pp. 643–660, Jun. 2001.
- [28] K. C. Lee, J. Ho, and D. J. Kriegman, "Acquiring linear subspaces for face recognition under variable lighting," *IEEE Trans. Pattern Anal. Mach. Intell.*, vol. 27, no. 5, pp. 684–698, May 2005.
- [29] G. B. Huang, M. Ramesh, T. Berg, and E. Learned-Miller, "Labeled faces in the wild: A database for studying face recognition in unconstrained environments," Dept. Comput. Sci., Univ. Massachusetts, Amherst, MA, USA, Tech. Rep. 07-49, Oct. 2007.
- [30] Z. Guo, L. Zhang, and D. Zhang, "A completed modeling of local binary pattern operator for texture classification," *IEEE Trans. Image Process.*, vol. 19, no. 6, pp. 1657–1663, Jun. 2010.
- [31] B. Zhang, S. Shan, X. Chen, and W. Gao, "Histogram of Gabor phase patterns (HGPP): A novel object representation approach for face recognition," *IEEE Trans. Image Process.*, vol. 16, no. 1, pp. 57–68, Jan. 2007.
- [32] C. H. Chan, J. Kittler, N. Poh, T. Ahonen, and M. Pietikäinen, "(Multiscale) local phase quantisation histogram discriminant analysis with score normalisation for robust face recognition," in *Proc. 12th Int. Conf. Comput. Vis. Workshops*, Oct. 2009, pp. 633–640.
- [33] X. Tan and B. Triggs, "Enhanced local texture feature sets for face recognition under difficult lighting conditions," *IEEE Trans. Image Process.*, vol. 19, no. 6, pp. 1635–1650, Jun. 2010.
- [34] S. H. Lee, J. Y. Choi, Y. M. Ro, and K. N. Plataniotis, "Local color vector binary patterns from multichannel face images for face recognition," *IEEE Trans. Image Process.*, vol. 21, no. 4, pp. 2347–2353, Apr. 2012.
- [35] C. Liu and H. Wechsler, "Gabor feature based classification using the enhanced Fisher linear discriminant model for face recognition," *IEEE Trans. Image Process.*, vol. 11, no. 4, pp. 467–476, Apr. 2002.
- [36] D. Zhang, W. K. Kong, J. You, and M. Wong, "Online palmprint identification," *IEEE Trans. Pattern Anal. Mach. Intell.*, vol. 25, no. 9, pp. 1041–1050, Sep. 2003.
- [37] L. Wolf, T. Hassner, and Y. Taigman, "Similarity scores based on background samples," in *Proc. Asian Conf. Comput. Vis.*, 2009, pp. 1–5.



**Kuo-Chin Fan** was born in Hsinchu, Taiwan, in 1959. He received the B.S. degree in electrical engineering from National Tsing Hua University, Hsinchu, in 1981, and the M.S. and Ph.D. degrees from the University of Florida, Gainesville, FL, USA, in 1985 and 1989, respectively. He then joined the Institute of Computer Science and Information Engineering, National Central University, Zhongli, Taiwan, where he became a Professor in 1994. He was the Chairman of the Department from 1994 to 1997 and the Vice President of Fo Guang University, Yilan, Taiwan, from 2007 to 2011. He is currently the Chair Professor with the Institute of Computer Science and Information Engineering, National Central University. He was a recipient of three consecutive Distinguished Research Fellow Awards from the National Science Council, and was a Life Distinguished Research Fellow in 2011. His research interests include image analysis, biometric verification, and video surveillance.



**Tsung-Yung Hung** was born in Changhua, Taiwan, in 1984. He received the B.S. and M.S. degrees in computer science and information engineering from National Central University, Zhongli, Taiwan, in 2008 and 2010, respectively, where he is currently pursuing the Ph.D. degree. His research interests include image processing, pattern recognition, and machine intelligence.